P5.10 MICROWAVE SIMULATIONS FROM GROUND-BASED SOUNDINGS AND COLLOCATED OBSERVATIONS FROM SATELLITES: A TRIAL STUDY FOR DMSP/SSMIS CALIBRATION/VALIDATION

Ye Hong*, John Wessel, and Robert Farley
The Aerospace Corporation
Los Angeles, CA 90009

1. INTRODUCTION

The first Defense Meteorological Satellite Program (DMSP) Special Sensor Microwave Imager/Sounder (SSMIS) is scheduled to be launched in May 2003. The SSMIS is a next-generation passive conically scanning microwave radiometer that combines both imaging and sounding capabilities of current operational instruments, SSM/I, SSM/T-1 and SSM/T-2. It also improves the capability of temperature sounding by providing profiles from the surface up to 70 km altitude with higher spatial resolutions (~37.5 km for lower air and ~75 km for upper air). The SSMIS Calibration/Validation (Cal/Val) campaign is being conducted in order to verify performance of the instrument and retrieval algorithms.

Several dry-runs of SSMIS Cal/Val have been carried out to prepare for post-launch Cal/Val. One of them was conducted in April 2002. The primary objective was to evaluate the accuracy of radiative transfer calculations as a means of calibrating sounding channels. This paper presents microwave simulations from lidar measured and model generated atmospheric profiles. The comparison between the simulations and collocated observations from satellites for the SSMIS sounding channels will be discussed.

2. DATA

As a part of the SSMIS Cal/Val campaign, a transportable lidar developed by The Aerospace Corporation was deployed at Barking Sands, Kauai. Temperature and water vapor profiles were measured during the period from April 10 to April 26, 2002. Vaisala RS-90 radiosondes profiled temperatures from the surface to 33 km altitude and lidar extended the profiles to 75 km. Collocated and coincident satellite data from SSM/I, SSM/T-1 (T1), SSM/T-2 (T2) and AMSU were collected at the Air Force Weather Agency (AFWA). Figure 1 displays the lidar site and an example of overpass T2 data.

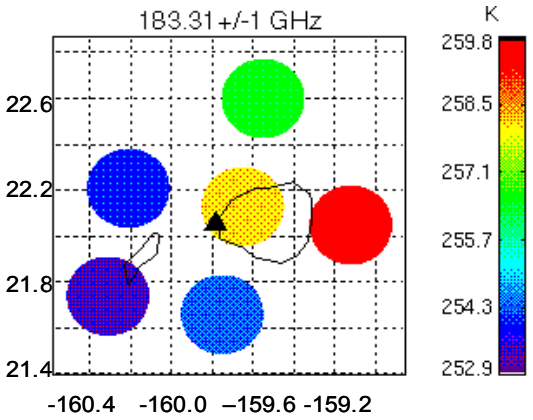

Figure.1 Lidar site (triangle) and samples of SSM/T-2 overpass data (circles).

For details of The Aerospace Corporation lidar one is referred to Farley and Wessel (2002), Wessel et al. (2000), and for the passive microwave radiometers on DMSP satellites to Grody (1993) and Falcone et al. (1992). Table 1 lists available collocated lidar, T1 and T2 data for the dry-run.

Table 1. Collocated Datasets

Date	Lidar Data			Satellite Data	
	Surf Temp (K)	No. of Levels	TWV (MM)	SSM/T1 (SAT/ORB1/ ORB2)	SSM/T2 (SAT/ ORB1/ ORB2)
4/10	296.2	138	41.39	F15/12015/12022	No Data
4/11	296.3	139	31.63	F15/12036	No Data
4/12	296.3	142	31.87	F15/12050	No Data
4/13	296.0	144	29.31	F15/12057/12064	No Data
4/18	297.3	136	32.62	No Data	F14/25989/25996 F15/12128/12135
4/19	298.0	141	30.73	F15/12149	F14/26003/26010 F15/12142/12149
4/20	297.0	139	35.30	F15/12163	F15/12156/12163
4/25	297.0	138	25.42	F15/12227	F14/26088 F15/12227

* Corresponding author address: Ye Hong, The Aerospace Corporation, M4-927, PO Box 92957, Los Angeles, CA 90009-2957; e-mail: Ye.Hong@aero.org

Collocated temperature and water vapor profiles from the operational RAdiosonde OBservation (RAOB) network as well as numerical weather predication (NWP) models, such as Aviation model (AVN) and Navy Operational Global Atmospheric Prediction System (NOGAPS), were also obtained from AFWA to provide broader spatial and temporal coverage. Figure 2 shows the temperature profiles from lidar, AVN and NOGAPS, respectively, on April 15, 2002. Note that atmospheric profiles from NWP models include data up to 10mb (~30km) while lidar measurements provide data up to 70km.

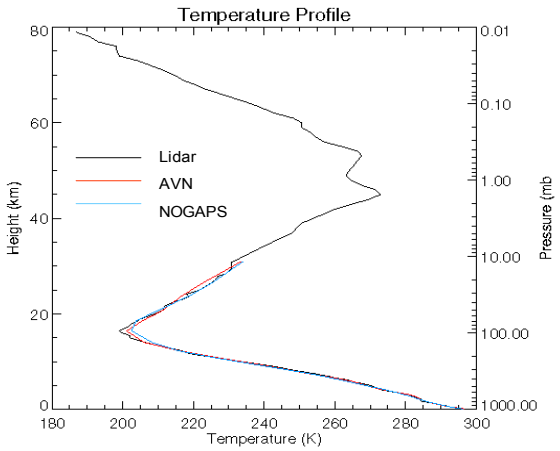

Figure 2. Temperature profiles from lidar, AVN and NOGAPS.

3. METHODOLOGY

For a non-scattering atmosphere, the brightness temperature observed by a satellite can be expressed as (Grody, 1993):

$$Tb_p(\theta) = \sec\theta \int_0^\infty \kappa(z)T(z)e^{-\tau(z,\infty)\sec\theta}dz + \varepsilon_{s_p}(\theta)Te^{-\tau(z,\infty)\sec\theta} +$$

$$[1-\varepsilon_{s_p}(\theta)][T_{cb}e^{-\tau(0,\infty)\sec\theta} + \int_0^\infty \kappa(z)T(z)e^{-\tau(0,z)\sec\theta}dz]e^{-\tau(z,\infty)\sec\theta} \quad (1)$$

where $T(z)$ is the atmospheric temperature at the altitude z, κ and τ are, respectively, the absorption coefficient and opacity due to atmosphere, ε_s and T_s are surface emissivity and temperature respectively, T_{cb} is the cosmic background with an approximate value of 2.7K, θ is the nadir angle, and the subscript, p, represents the polarization (vertical or horizontal).

Since the sounding instruments of T1 and T2 are cross-track radiometers, measured brightness temperatures are combinations of both vertical and horizontal signals depending on the nadir angle θ (Wessel and Boucher, 1998):

$$Tb(\theta) = Tb_h(\theta)\cos^2\theta + Tb_v(\theta)\sin^2\theta \quad (2)$$

where Tb_h and Tb_v are brightness temperatures for horizontal and vertical polarizations respectively.

A non-scattering radiative transfer model has been developed at The Aerospace Corporation to calibrate/validate the sounding channels of the SSMIS. The model can incorporate various atmospheric absorption models and surface emissivity models. If not specifically mentioned in the next section, Rosenkranz's water vapor absorption model (Rosenkranz, 1998) and oxygen absorption model (Rosenkranz, 1993) are applied. For ocean surface emissivity, the dielectric constant model by Stoygn et al (1995) and the specular reflectivity model with corrections for sea surface roughness (Wilheit, 1977, Stogryn, 1972 and Holinger, 1971) are used.

Radiative transfer calculations were performed for lidar and RAOB profiles as well as NWP model profiles for various nadir angles. The pixel number, provided with collocated T1 and T2 data, was used to derive the nadir angle for that pixel. Simulated brightness temperatures, derived from Equations (1) and (2), are then compared with observed T1 and T2 Sensor Data Records (SDRs).

4. RESULTS

Since the lidar site is near an island, an overpass satellite pixel usually covers both land and ocean regions. Thus channels that have contributions from surface are not considered here. Simulation results for channels 1-3 (183.31+/-1, 3, and 7 GHz) for T2 and channels 3-7 (54.35, 54.9, 58.4, 58.825 and 59.4 GHz) will be discussed.

Although high quality lidar data were available for about 10 days in April 2002, satellite data was not available for all overpasses. Also the NWS RAOB data was not

available at overpass times. Results below are from limited collocated data listed in Table 1.

4.1 SSM/T-1 Simulations

Figure 3 shows the scatter plot between simulations and observations for T1. Data from the T1 overpass were collected within a 300 km radius centered at the lidar site. In order to minimize the effect of displacement, only simulations from pixels that are the closest to the lidar site (usually < 100 km) for each overpass are displayed in Fig. 3.

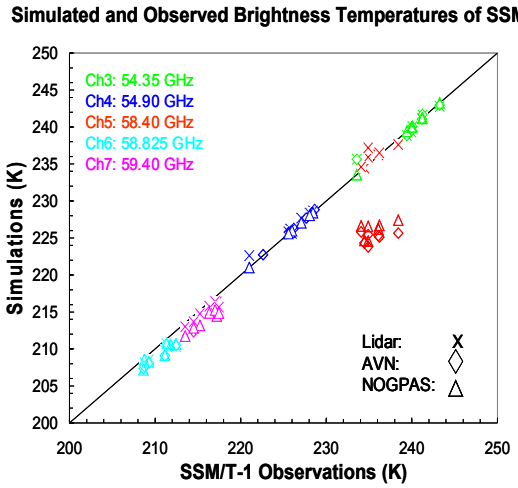

Figure 3. Comparison of SSM/T-1 simulations and observations.

It can be seen that simulations from lidar profiles agree with T1 observations very well. Also, T1 simulations from AVN and NOGAPS profiles are consistent with observations except for channel 5. Underestimation of channel 5 brightness temperatures is due to the upper boundaries of AVN and NOGAPS data at 10mb. Since the temperature weighting function for channel 5 peaks at about 10mb, the contributions arising from the atmosphere above 10mb are not accounted for.

4.2 SSM/T-2 Simulations

The scatter plot between simulations and observations for T2 is presented in Figure 4. Similar to T1, only simulations from pixels that are the closest to the lidar site (usually < 40 km) for each overpass are displayed.

It can be seen that T2 simulations from lidar profiles (crosses in Fig.4) agree with observations very well for channel 3 and reasonably well for channels 1 and 2. Due to the high variability of water vapor, discrepancies between simulations from AVN and NOGAPS are large (not shown). The biggest discrepancy is for channel 2 (183.31+/-1 GHz), for which the weighting function peaks at a higher altitude than the other two channels.

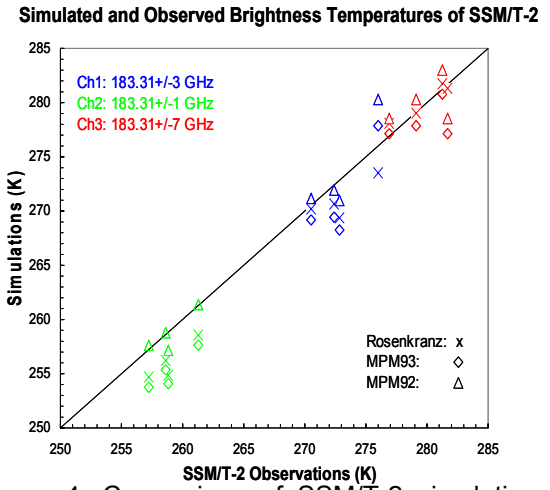

Figure 4. Comparison of SSM/T-2 simulations and observations.

Two other atmospheric absorption models, MPM92 (Liebe et al., 1992, Liebe and Hufford, 1989) and MPM93 (Liebe, 1993) have been applied in radiative transfer calculations for comparison (triangles for MPM92 and diamonds for MPM93 in Fig. 4). It appears that simulations using MPM92 match the observations best for the water vapor channels.

5. SUMMARY

One dry-run of SSMIS Cal/Val was conducted by The Aerospace Corporation in April 2002 to prepare for post-launch Cal/Val and to evaluate the accuracy of radiative transfer calculations for sounding channels. Temperature and water vapor profiles were measured by the Aerospace lidar deployed at Kauai. Collocated and coincident satellite data from SSM/I, SSM/T-1 (T1), SSM/T-2 (T2) and AMSU, as well as RAOB data and NWP model data were collected at AFWA.

Radiative transfer calculations from measured and model-generated atmospheric profiles were performed. Simulations from lidar, AVN and NOGAPS profiles agree with T1 observations very well. Although T2 simulations from lidar agree with satellite observations reasonably well, there are large discrepancies between observations and simulations from AVN and NOGAPS. Applications of three

atmospheric absorption models indicate that results from MPM92 best fit the observations for water vapor sounding channels.

It is apparent that data in the current study are inadequate to support firm conclusions with respect to the validity of water vapor absorption models. However, the existing measurements provide excellent support for the oxygen absorption model and represent a good start for the Cal/Val campaign.

ACKNOWLEDGMENTS

The authors would like to thank Mr. Bruce Thomas and Dr. James Drake for collecting collocated satellite, RAOB and NWP model data. The first author would also like to thank Drs. Chris Kummerow of Colorado State University, Guosheng Liu of Florida State University and Fuzhong Weng of NOAA/NESDIS for their help on radiative transfer modeling. This work was supported by the DMSP Program Office.

REFERENCES

Farley, R. W. and J. E. Wessel, 2002, Lidar atmospheric profiles from Barking Sands, Kauai, *Maui/MALT Workshop, Hawaii*, Sept.14, 2002

Falcone et al., 1992: SSM/T-2 calibration and validation data analysis, *Phillips Laboratory, Hanscom AFB, MA, Tech. Rep*. 92-2293.

Grody, N. C., 1993: Remote sensing of the atmosphere from satellites using microwave radiometry, in *Atmospheric Remote Sensing by Microwave Radiometry*, M. A. Janssen, Ed. New York: Wiley, Ch. 6.

Hollinger, J. P., 1971: Passive microwave measurements of sea surface roughness, *IEEE Trans. Geosci. Remote Sensing*, **GE-9**, 165-169.

Liebe, H. J., and G. A. Hufford, 1989: Modeling millimeter-wave propagation effects in the Atmosphere, *AGARD CP-454,* October, 1989, paper 18.

Liebe, H. J., G. A. Hufford and M. G. Cotton, 1993: Propagation Modeling of Moist Air and Suspended Water/Ice Particles at Frequencies Below 1000 GHz, *AGARD CP-542,* May 1993, paper 3.

Liebe, H. J., P. W. Rosenkranz and G. A. Hufford, 1992: Atmospheric 60-GHz oxygen spectrum: New measurements and line parameters, *J. Quant. Spectr. Radiat. Tr.,* **48,** 629-643

Rosenkranz, P. W. 1993, Absorption of microwaves by atmospheric gases, in *Atmospheric Remote Sensing by Microwave Radiometry*, M. A. Janssen, Ed. New York: Wiley, Ch. 2.

Rosenkranz, P. W. 1998, Water vapor microwave continuum absorption: A comparison of measurements and models, *Radio Sci.,* **33,** 919--928.

Stogryn, A., 1972: The emissivity of sea foam at microwave frequencies, *J. Geophys. Res*., **77**, 1658-1666.

Stogryn, A. P., H. T. Bull, K. Rubayi, and S. Iravanchy, 1995: The microwave permittivity of sea and fresh, Aerojet Report, GenCorp Aerojet, Azusa, CA.

Wessel, J. E. and D. Boucher, Jr., 1998: Comparison between cross-track and conical scanning microwave window channels near 90 GHz, *IEEE Trans. Geosci. Remote Sensing*, **36**,16-24.

Wessel, J. E., S. M. Beck, Y. C. Chan, R. W. Farley and J. A. Gelbwachs, 2000: Raman lidar calibration for the DMSP SSM/T-2 microwaver water vapor sensor. *IEEE Trans. Geosci. Remote Sensing*, **38**,141-154.

Wilheit, T. T., 1979: A Model for the Microwave Emissivity of the Ocean's Surface as a Function of Wind Speed, *IEEE Trans. Geosci. & Elec.*,**GE-17,** 244-249.